Ocean circulation from altimetry: progresses and challenges

Yongsheng Xu *
Jackson School of Geosciences, University of Texas at Austin

Jianke Li
College of Marine Science, University of South Florida

Shenfu Dong
The Cooperative Institute for Marine and Atmospheric Studies, University of Miami

*Corresponding Author email: xu@geo.utexas.edu

ABSTRACT

The paper provides a review of recent progresses in physical oceanography, such as results on studying ocean circulation and mesoscale ocean dynamics derived from satellite altimetry. Since 1992, satellite altimetry has provided an unprecedented 16 years monitoring of sea level and ocean circulation variations. Continuous measurements from satellites like TOPEX/Poseidon and Jason-1 help us understand and foresee the effects of the changes in ocean circulation on climate and on extreme climate events such as El Niño and La Niña. Altimeter measurements have improved our understanding of both the dynamics and thermodynamics of western boundary currents by providing a synoptic view of the current systems and their interannual variations, and allowed scientists to quantify eddy-induced salt and heat transport, and seasonal and interannual variations in eddy kinetic energy. Altimeter measurements have also been used to map eddies, quantify their amplitudes and diameters, track their trajectories, and examine their eddy dynamics and roles in the ocean processes and climate variability. Recent advances in satellite altimetry, in synergy with other remote sensing techniques, constrain the uncertainty of mechanic energy driving meridional overturning circulation which regulates climate change. Moreover, altimetry has discovered a surprising sea level anomaly propagation speed which challenges the existing linear Rossby wave theory, and revealed the presence of elusive zonal fronts and jets in the ocean.

However, challenges still exist in monitoring the ocean variability from satellite altimetry. Satellite altimeters are not able to measure the time-mean geostrophic currents due to the large uncertainty in geoid. This poses challenges for deriving the absolute geostrophyic flow in regions where bottom velocities are non-zero since hydrographic estimates of absolute dynamic topography are unable to capture the effects of the bottom. The uncertainties of satellite altimetry

measurements have a high geographic variability. The existence of high frequency energetic barotropic motions in the ocean can lead to a large aliasing error in satellite altimetric observations. New evidences show that the combined aliasing from several neighboring and crossing tracks could produce unreal mesoscale signals in altimeter mapped product. Although satellite altimetry has improved our understanding of the climate system dramatically, it is important to keep in mind that problems still remain and new challenges will arise.

1. INTRODUCTION

The ocean plays a key role in the global climate variability. To understand ocean's role and subsequently develop techniques for predicting future climate, one must understand the dynamics of the global ocean circulation, that is the movement of water that transports mass, heat, salt, and other biogeochemical properties of the ocean that are closely linked to the processes of climate change. Before satellite altimeter missions, most knowledge of the global ocean circulation has been pieced together from spatially and temporally scattered observations, which are not adequate for a quantitative description of either the mean or the time-varying components of the global ocean circulation. The only viable approach to observe the surface circulation of the global ocean with sufficient resolution and consistent sampling is the use of a satellite radar altimeter to measure the height of the sea surface [Wunsch and Gaposchkin, 1980; Stewart, 1985; Wunsch, 1992].

Satellite altimeter is a remote sensing sensor providing an integrated picture of the oceans over large spatial and temporal extents. A satellite altimeter is a nadir pointing active microwave sensor designed to measure characteristics of the surface of the earth. The return signals from oceanic regions provide a range measurement from the satellite to the sea surface immediately below. After removing the effects of the tides and atmospheric pressure from the observation, the deviation of the sea surface from the geoid, i.e., ocean dynamic topography, is related to the velocity of the surface geostrophic flow - a component of the surface flow on which the surface pressure force is balanced by the Coriolis force due to the Earth's rotation. The major ocean currents can raise sea surface height (SSH) by up to a meter higher than the surrounding area. The ocean dynamic topography provides a strong constraint for determining the ocean circulation through the entire water column via the dynamic equations governing the fluid

motion. Precise measurement of the shape of the global sea surface thus provides a powerful tool for studying the dynamics of the ocean circulation.

Over the last two decades, satellite altimetry has provided a global, high-resolution, regular monitoring of sea level and ocean circulation variations. The early satellite altimetry missions such as SEASAT (1978) and GEOSAT (1986-1989) provided the first global coverage of the sea level variations. In the early 1990s, among the numerous accomplishments is a powerful methodology developed by Kelly and Gille [1990] for estimating the absolute dynamic ocean topography across strong currents from their temporal variabilities. An analytical model is used to describe the dynamic topography of an isolated jet with its kinematic parameters (i.e., location, width, and amplitude) determined from the observed temporal sea level changes as an inverse problem (also see *Tai*, [1990]). Comparison of the altimetry-derived velocities with simultaneous in-situ velocity measurements demonstrated the validity of the technique [*Joyce et al.,* 1990]. The position and strength of meandering jets were monitored in the Gulf Stream [Kelly and Gille, 1990], the Kuroshio [Qiu, 1992] and the Antarctic Circumpolar Current (ACC) [Gille, 1994]. A review of the early studies can be found in [Le Traon and Morrow, 2001].

There is a long history of development in satellite altimetry before reaching the performance of TOPEX/POSEIDON (hereafter T/P) which was launched in 1992 with a 10-day repeat cycle. The root-mean-square (rms) uncertainty in the SSH measurement relative to the earth's center is 4.7 cm (including errors in both orbit determination and altimeter measurement) (Fu et al. 1994), which is time dependent and can be reduced to about 2 cm by time averaging. Multi-mission period was underpinned by the very precise T/P mission and its follow on mission Jason-1 which was launched in 2001. At the same time, ERS-1 (1991-1995), ERS-2 (1995-2005) and ENVISAT (2002 ->) were in orbit providing a better spatial coverage on a 35-day repeat. The

complementary sampling of two or more altimeter missions provides precise measurements needed to monitor ocean mesoscale variability [Le Traon and Morrow, 2001]. Moreover, the progress in multi-mission mapping technique enables altimeter to resolve mesoscale variability with space scales of 50-500 km, time scales of 10-100 days, and currents of a few km/h. These mesoscale variability are the principal mechanism for the poleward transport of heat across strong zonal currents, such as the ACC [Karsten and Marshall, 2002; Jayne and Marotzke, 2002]. Remote sensing from satellites has been established as one of the most practical approaches to observe the global ocean with adequate space and time resolution.

In the following sections we will present some of the exciting advances in physical oceanography since T/P mission. For a comprehensive review of previous studies, the reader is referred to [Le Traon and Morrow, 2001].

2. MULTI-MISSION MAPPING

In many ways, the orbit design of an altimetry satellite is a compromise. But one point that deserves special attention is to get the right balance between spatial and temporal resolution: a satellite that revisits the same spot frequently covers fewer points than a satellite with a longer orbital cycle. One solution to achieve high resolution coverage is to operate several satellites together. Merging multisatellite data sets open a door to resolve the main space scales and time scales of the ocean circulation, in particular, the mesoscale. Combining different altimetric missions is a delicate task: since each mission has different error budgets and orbit differences, leading to large-scale biases and requiring trends to be corrected. It has been shown that homogenous and intercalibrated SSH data sets can be obtained by using the most precise mission (T/P and, later on, Jason-l) as a reference for the less precise missions [Le Traon et al., 1995; Le Traona and Ogor, 1998]. Ducet and Le Traon [2000] gave the first results of the global mapping

of sea level and ocean circulation variations from the combination of T/P with ERS-1 and ERS-2. The mapping of the ocean signal was done globally through an improved objective analysis method that takes long wavelength residual errors into account and uses realistic correlation scales of the ocean circulation with a global high-resolution of ¼ degree every 10 days. To reduce measurement noise, sea level anomaly (SLA) is filtered and subsampled. SSALTO/DUACS project applied the sub-optimal interpolation technique to construct gridded data sets from multi-mission altimeter data [Le Traon and Dibarboure, 2002]. Before mapping, a crossover analysis is applied to minimize the errors between groundtracks, including a correction for the large-scale orbit errors. All of the available altimetric data is then mapped onto a regular 1/3° grid every 7-10 days.

Fig. 1 shows the rms variability of the SLA obtained from T/P data only and from the combined altimeter data. Unrealistic features on the T/P map exist mainly in the regions with high variability, where the rms changes erroneously from one grid point to the next (upper panel, Fig 1). The large intertrack distance of T/P (2.8^{o}) does not allow an adequate mapping of the mesoscale ocean circulation variability. However, combining T/P with ERS data resolves the mesoscale variability (lower panel, Fig 1). Furthermore, the eddy kinetic energy (EKE) from the merged T/P + ERS-1 and ERS-2 maps is 30% higher than that from T/P maps alone. The merged maps also produce realistic global estimates of zonal and meridional components of EKE and their seasonal variations, which can be used to better identify EKE sources. A comparison of velocity statistics with World Ocean Circulation Experiment surface drifters in the North Atlantic shows a good agreement [Ducet and Le Traon, 2000].

Although the T/P+ERS merged data provide a very good representation of the mesoscale variability, the remaining error can be quite important especially for correctly determining the

velocity field in coastal and mesoscale situations [Greenslade et al., 1997; Tai, 1998]. Since mid-September 2002, there is an exceptional sampling of the ocean with four altimeter missions flying simultaneously [Jason-1, ERS-2/ENVISAT, T/P interleaved with Jason-1 and Geosat Follow-On (GFO)]. These data sets were merged to improve the estimation of mesoscale surface height anomaly in the Mediterreanean Sea as shown in Fig. 2. It can be seen that with four altimetry satellites available, the resolution of SSH measurements is greatly enhanced. On average, the merged Jason-1 + ERS-2 + T/P +GFO maps yield EKE levels 15% higher than Jason-1 + ERS-2. The consistency between altimetry and sea surface temperature, drifting buoys and tide gauges, is also significantly improved when four satellites are merged compared to the results derived from the two-satellite configuration [Pascual et al., 2005]. Other combinations are possible. There is no doubt that multi-mission mapping is a significant step forward for studying the mesoscale ocean circulations (mesoscale eddies) since it first brought World Ocean eddies into focus.

3. MESOSCALE EDDIES

Satellite altimetry has made a unique contribution to observing and understanding mesoscale eddies. We now have more than 20 years of good mesoscale variability measurements from Geosat (1986-1989), ERS-1 and ERS-2 (1991-2008), T/P (1992-2005), and Jason-1 (2001-2008) to learn more about the seasonal/interannual variations in mesoscale variability intensity. Analyses of altimeter data have produced global, quantitative estimates of eddy energy with high spatial resolution, revealing details such as the correlation of EKE with the mean currents and the role of topography and winds. From satellite altimeters, mesoscale eddies can be observed almost everywhere in the mid and high latitudes. Their energy generally exceeds the energy of

mean flow by an order of magnitude or more (e.g, Wyrtki *et al*., 1976; Richardson, 1983; Schmitz and Luyten, 1991).

Merged datasets from multiple altimeters greatly improved ability of resolving mesoscale eddies (Chelton and Schlax, 2003; Fu *et al*., 2003; Pascual *et al*., 2006). In Fig 1 (lower panel), the rms sea level variability in western boundary currents (Gulf Stream, Kuroshio, Brazil-Malvinas Confluence, Agulhas) and the ACC (Fig.1, lower panel) is higher than 30 cm and can reach up to 50 cm. The maximum eddy variability is observed in the Agulhas region, followed by the Gulf Stream, Kuroshio, and Confluence regions and finally by the ACC. EKE (Fig. 3) has been used to represent mesoscale signals because it is much less sensitive to large scale signals than the variance of SLA (Fig. 1). As expected, the strong EKE is concentrated in the vicinity of the major current systems, and its magnitude can reach up to 4500 $cm^2\ s^{-2}$. The maximum value is in the Agulhas region, with secondary maxima in the Kuroshio, the Gulf Stream, the Brazil/Malvinas Confluence zone, and finally, the ACC. Stammer (1997) showed that there is a good correspondence between EKE and mean kinetic energy (MKE), which confirms that the currents are the main sources of eddies. In the ACC, high mesoscale variability is also found in regions of abrupt changes of bottom topography and do not appear to be associated with strong mean currents. This may simply imply that in these areas, baroclinic instability is unlikely to occur and that other mechanisms are to be sought (e.g., barotropic instability, mean current/bottom topography interaction).

Stammer and Wunsch (1999) investigated the seasonal and interannual variations in eddy energy using 4 years of T/P data. Over most of the subtropical regions and along major ocean fronts, the variations are weak and often negligible. Western boundary current extensions show an annual cycle, with a maximum occurring in late summer/early falls. A pronounced annual

cycle in eddy energy was also apparent in the eastern North Pacific and the northern and eastern North Atlantic. In these regions, Stammer and Wunsch (1999) found a significant correlation between EKE and wind-stress forcing at seasonal and interannual time scales. Using 8 years of combined T/P and ERS-1/2 altimeter data, Brandt *et al.* (2004) investigated the seasonal to interannual variability of the eddy field in the Labrador Sea. The mean EKE shows strong seasonality, and the interannual variability shows distinct regional differences.

Stammer (1998) and Stammer *et al.* (2006) estimated the meridional eddy heat and salt transport for the global ocean using T/P altimeter data. Strong poleward eddy heat and salt transport occur in the energetic western boundary currents: The Gulf Stream, the Kuroshio, and the Agulhas Current. In the equatorial band (5^{o}N to 5^{o}S), eddy heat and salt flux are northward in the Pacific and southward in the Indian Ocean, while equatorward eddy transport occurs between 5^{o} and 20^{o} latitude. Qiu and Chen (2005) investigated the eddy-induced heat transport in the Subtropical North Pacific in the Kuroshio Extension region using 6 years of merged T/P and ERS-1/2 altimeter data. The meandering zonal jet is found to generate opposite sign eddy heat fluxes. As a result, the zonally integrated poleward heat transport associated with the Kuroshio Extension is at a level *O* (0.1 PW), smaller than the previous estimates based on turbulent closure schemes. Large poleward eddy heat transport is also found in the subtropical North Pacific along a southwest–northeast-tilting band between Taiwan and the Midway Islands.

Isern-Fontanet *et al*. (2003; 2006) developed a procedure to detect individual eddies. In this method, Eddies were identified by closed contours of the Okubo-Weiss parameter, W, which is a measure of the relative importance of deformation and rotation and is given by the sum of the squares of the normal and shear components of strain minus the square of the relative vorticity (Refer Isern-Fontanet *et al*. 2003, 2006 for details). With this method and using 10-year period of

merged T/P and ERS-1/2 altimeter datasets, Chelton *et al.* (2007) investigated the global eddy characteristics. Their analyses showed that mean eddy amplitudes (Fig. 4b) range from only a few cm in the low-energy regions to more than 20 cm near strong currents. Generally, both the eddy density and the mean eddy amplitude are largest in regions of large SSH variance; few tracked eddies were detected in regions where the filtered SSH standard deviation is less than 4 cm. The mean eddy diameters as defined by the chosen W contour decrease from about 200 km in the eddy-rich low and middle latitudes to about 100 km at high latitudes (Fig 4c). This factor-of-2 decrease in diameters is similar to the eddy scales noted previously from much higher-resolution along-track altimeter data [Stammer, 1997], but is smaller than latitudinal decrease in the Rossby radius which is often associated with eddy size. Such large eddy sizes relative to the Rossby radius have also been noted from in situ data in the subtropical North Pacific [Roemmich and Gilson, 2001]. Analysis by Scott and Wang (2005) supports this view. Based on altimetric estimates of spectral kinetic energy flux, they argued that there is evidence for an upscale nonlinear cascade of kinetic energy with an arrest scale similar to the large eddy diameters obtained here.

Another striking characteristic of the eddy trajectories is the strong tendency for purely westward propagation. For over 1300 long-lived cyclonic and anticyclonic eddies with lifetimes exceeding 12 weeks, only about 1/4 had mean propagation directions that deviated by more than 10^{o} from due west. Cyclonic and anticyclonic eddies have preferences for small poleward and equatorward deflections, respectively. Similar results have previously been obtained regionally [Morrow *et al.*, 2004]. Eddy speeds equatorward of about 25^{o} are slower than the zonal phase speeds of nondispersive baroclinic Rossby waves predicted by the classical theory. In the Antarctic Circumpolar Current, nearly all of the eddies are advected eastward. Elsewhere, eddy

speeds are similar to the westward phase speeds of classical Rossby waves. The propagation speeds and directions of the observed extratropical eddies are consistent with theories for nonlinear vortices, implying the nonlinearity of the majority of global ocean eddies.

Despite all this progress, there is still much to learn from altimeter data for mesoscale variability. The evolvements of the energy, including potential energy and kinetic energy, and the vorticity of individual eddies are not yet well understood and systematic studies of individual eddies need to be conducted further. Because of the sampling requirements in both space and time, distinguishing between Rossby waves and eddies is difficult and the relation between them needs to be better analyzed. The combined use of altimeter data with *in situ* data (*T* and *S* profiles, drifters, floats) and forcing data should also be developed further for a better understanding of mesoscale variability dynamics. Without *in situ* data a three-dimensional description of mesoscale eddies would be impossible. Assimilation into models is a powerful means for performing such integration.

4. OCEAN TIDES

The accurate global measurements of the ocean tides by T/P allow addressing some longstanding questions that have wide-ranging implications for physical oceanography. Two major tidal achievements attribute to advent of high accurate global altimeter missions are progresses in understanding tidal energy dissipation and internal tide. These results have triggered a huge new interest in the role of tides in controlling the ocean circulation and more generally in the question of the ocean circulation energetics.

The problem of how and where the tides dissipate their energy was listed by Wunsch [1990, p. 69] as one of four "significant hard problems [in physical oceanography] to be solved in the next century." The advances in tidal mapping provided by high accurate T/P have finally allowed

people to investigate the nature and the location of tidal energy dissipation. Using satellite altimeter data from T/P to map empirically the tidal energy dissipation, Egbert and Ray [2000, 2001] reported that about 25 to 30% of the global energy dissipation, or about 1 terawatt (1 trillion watts), occurs in the open ocean. Fig 5 indicates significant dissipation in the deep ocean, especially near rugged bottom topography such as Hawaiian Ridge. One important implication of this finding concerns the possible energy sources needed to maintain the ocean's large-scale "conveyor-belt" circulation and to mix upper ocean heat into the abyssal depths. It is thought that 2 terawatts are required for this process. The wind power input to the oceanic general circulation was found to be about 1 terawatt using satellite data [Xu and Scott, 2008a; Wunsch 1998; Scott and Xu, 2008]. Now people find another energy source to supply the remainder: the deep sea tidal energy dissipation.

T/P data also reveal the presence of coherent internal tides in many places throughout the ocean. The small amplitudes of the internal tides require very long time series of sea level observations to extract them from a background of larger oceanographic signals and noise. As T/P is supplemented by the Jason-1 time series, these data become more valuable for tide studies. Internal tides can be observed in altimetry as small (usually less than 2 cm), short-wavelenth (150 km) modulations in the tidal surface elevations. They are most easily observed in along-track tidal estimates [Ray and Mitchum, 1996 and 1997]. By fitting monochromatic plane waves to subdomains of the altimeter data, Ray and Cartwright [2001] showed satellite data enable direct mapping of internal-tide sources, sinks, and power transmission routes throughout the ocean. Fig 6 shows energy flux vectors of the M_2 first-mode internal tide throughout the central North Pacific Ocean derived by Ray and Cartwright [2001]. Internal wave energy is observed transporting to both north and south from the Hawaiian Ridge, sometimes in remarkably narrow

beam patterns. A very localized source along the Aleutian Ridge generates waves that propagate southwards over 2000 km.

The advances in tidal mapping provided by T/P have finally allowed us to begin to answer some longstanding questions about tidal energetics. As we know about 25 to 30% of the global energy dissipation occurs in the open ocean. Many of barotropic dissipation regions are identical to the internal-tide sources. The mechanism at work is almost certainly the scattering of surface wave energy into internal tides and other baroclinic motions. It is thus conceivable that the dissipation of tidal energy is intimately related to the vertical mixing of the ocean and to its thermohaline circulation. It is possible that tidally induced ocean mixing, with a proper representation, may have important implications for long-term climate modeling. The satellite observation of ocean tides has indeed triggered a huge new interest in the role of tides in controlling the ocean circulation and more generally in the question of the energetics of the circulation.

5. OCEAN CLIMATE VARIABILITY

The ocean is permanently in motion and exchanges large amount of heat with the atmosphere, thus playing a major role in climate. It is responsible for about half of the total poleward heat transport in the Earth system. From the seasonal to the decadal, or even the centennial timeframe, the ocean's influence upon the atmosphere is one of the keys to understand and predict the climate variability. Better knowledge of ocean circulation is enabling us to better understand and predict climate variability. Altimetry is one of the most important tools for monitoring ocean dynamics, and as such is a source of vital data to include in forecasting models of ocean-atmosphere coupled events such as El Niño, monsoons, the North Atlantic Oscillation or decadal oscillations.

El Niño (La Niña) refers to a sequence of changes in circulations across the equatorial Pacific Ocean and Indonesian archipelago when warming is particularly strong (weak). Space-based altimeter platforms have provided unprecedented perspective of global ocean. An excellent example of this is the extreme changes that have been observed in tropic Pacific during the evolution of El Niño and the subsequent La Niña as shown in Fig 7. From February to April 1997, T/P satellite data pinpointed a large eastward-moving swelling of waters in the central Pacific. This positive sea-level anomaly, over 10 cm and increasing with time, peaked near the South America Coast. In July 1997, the signature was plain and south-east Asia was hit by severe drought. The anomaly in red on the map, corresponding to "extra" warm waters, covered an area 1.5 times of the United States. By June 1998, surface height was returning to normal. In July 1998, T/P revealed favorable conditions for La Niña, which developed in 1999. In 2000, ocean once more returned to normal. The satellite has continuously tracked related ocean-climate changes in the Pacific Ocean. In other low latitude region where there is not comprehensive in situ observation system, and in particular in Indian Ocean, altimeter is becoming the most important data stream to describe the large scale ocean circulation.

The Pacific Decadal Oscillation (PDO) is a long-term ocean fluctuation of the Pacific Ocean, similar to the El Niño/La Niña cycles but on a much larger scale. The PDO waxes and wanes approximately every 20 to 30 years. Causes for the PDO are still unknown. Cummins et al. [2005] have shown that the principal component of SSH anomaly from satellite altimeter can provide a robust index of regional climate variability that is less noisy than SST-based PDO index. Thus long term satellite altimeter data provides a powerful tool to help scientists to observe and understand the phenomenon. From T/P data (see below) together with other oceanic and atmospheric data, some scientists think we have just entered the 'cool' phase. The 'cool'

phase is characterized by a cool wedge of lower than normal sea-surface heights/ocean temperatures in the eastern equatorial Pacific and a warm horseshoe pattern of higher than normal SSH connecting the north, west and southern Pacific. In the 'warm' or 'positive' phase, which appears to have lasted from 1977- 1999, the west Pacific Ocean becomes cool and the wedge in the east warms.

Much of the heat transported poleward by the oceans is carried in the midlatitude western boundary currents in the northern hemisphere. The radar altimeter has made possible to increase understanding of both the dynamics and thermodynamics of western boundary currents. Observations of SSH anomalies from the T/P radar altimeter [Fu et al., 1994] since 1992 suggest that there are large interannual-to-decadal variations in the structure of these current systems [Qiu, 2000; Vivier et al., 2002; Dong and Kelly, 2004]. Imawaki [2001] showed that the Kuroshio transport could be monitored using SSH. Meanwhile, the relationship between SSH and heat content was probed by numerous researchers demonstrating that SSH was a good proxy for upper ocean heat content. In contrast to the traditional notion that changes in the westerlies cause corresponding changes in air-sea fluxes and therefore in the ocean heat content, Qiu [2000] showed using T/P data that large changes in heat content were the result of changes in the geostrophic heat advection in the kinetic energy (KE) rather than air-sea fluxes. Vivier et al. [2002] and Dong and Kelly [2004] further revealed that changes in upper ocean heat content were primarily the result of changes in heat transport by the geostrophic current with time scales of several years or more. Much of the anomalous heat transport is stored in the recirculation gyre regions, where heat accumulates and results in anomalous fluxes of heat to the atmosphere [Kelly and Dong, 2004]. Thus, interannual variations in air-sea fluxes in these regions are

primarily the result of changes in the ocean, not in the atmosphere. These results indicated the importance of ocean circulation in controlling climate variability.

6. PLANETARY WAVES

Though the major currents are very important, the ocean and climate are also influenced by phenomena that are more difficult to see. Large scale 'Planetary' waves cross the oceans and interact with general ocean circulation. These are either Rossby waves, which travel from east to west, or equatorial Kelvin waves which move in the opposite direction. They intensify currents such as the Gulf Stream or the Kuroshio. In addition, they may be reflected off the continents and return in the opposite direction, or follow coastlines. These waves and their reflections play a key role in the El Niño phenomenon. The existence of Rossby waves had been predicted theoretically for over 50 years, but they could not be observed until the advent of high-precision altimetry satellites. Their small amplitude (a few centimeters) and velocity (a few kilometers per day, depending on the latitude – for instance, they take several years to cross the Pacific Ocean at the 30° latitude), and large extent (an ocean basin) made it nearly impossible to observe using in situ measurements. High-precision altimetry is the best way of detecting these waves. Given the fact that Rossby waves travel almost zonally, they can be observed through a longitude-time plot (also known as a Hovmöller diagram) of the SSH, as shown in Fig 8. The waves can be seen clearly as diagonal (i.e. going from bottom right to top left) alignments of crests and troughs. The speed of propagation of the waves can be estimated from the slope those crests or troughs.

During the late 1970s and early 1980s there was considerable debate within the equatorial theoretical community regarding the existence and importance of the equatorial wave modes and the their role in remote forcing and El Niño. The launch of ERS-1 in 1991 and T/P in 1992 gave new impetus to the study of planetary waves by providing high-quality global time series of

SSH, which are continued by the Jason-1, ERS-2, Envisat and GFO missions. The space-time coverage of altimeter data unequivocally identified the existence of the equatorial waves via their propagation speed and horizontal structure. Analysis of altimeter data has shown that the reflection of equatorial Kelvin waves into Rossby waves at the eastern boundary and the associated perturbations to zonal advection are much more important in the evolution of the ENSO cycle and the related displacements of the warm pool than what was believed previously.

Another major discovery from altimetry data was that the sea level anomalies propagated westward with a wave speed up to twice as fast as that predicted from linear Rossby wave theory [Chelton and Schlax, 1996]. This observational discovery led to host of revised theories on Rossby wave propagation, which took into account the vertical shear in the background flow, bathymetric effects, etc [Killworth et. al, 1997; Killworth and Blundell, 2003] but for a review see Fu and Chelton [2001]. Although the difference between the propagation speeds from revised theories and from observed propagation has been reduced, the observed speeds remain faster than theoretical predicts.

7. SEA LEVEL CHANGE AND VARIABILITY

The measurement of long-term changes in global mean sea level can provide an important corroboration of predictions by climate models of global warming. Coastal tide gauges have provided the main technique by which sea level change has been measured during the past century. However, tide gauges are usually restricted to coastline and open sea island, and therefore do not adequately represent the global ocean. Satellite altimetry provides a means of overcoming the limitations of tide gauge measurements because the measurements are truly global in distribution and tied to the earth's center-of-mass in a well defined reference frame. Long term drift calibration of altimeters is essential for improving real estimate from altimeter

and assembling an uninterrupted record of sea level change from multiple instruments (e.g., T/P and Jason). Much effort has been done on it. Mitchum [1994, 1997, 1998 and 2000] and Chamber et al. [1998] have demonstrated that comparing sea level measurements from altimeter to tide gauges provides an effective way to determine the altimeter drift and the relative bias between two different instruments. Fig 9 shows a time series of the altimeter instrument behavior derived by Mitchum [2000] using these techniques. The abrupt change at the end of 1998 was due to switching to the redundant altimeter electronics on the satellite (side A to side B), so effectively T/P has used two separate instruments during its mission, each of which should be expected to have different behavior. Errors in determining the altimeter instrument drift using the tide gauges, currently estimated to be about 0.4 mm/yr, are almost entirely driven by errors in knowledge of vertical land motion at the gauges [Mitchum, 2000]. Future monitoring of the tide gauges using geodetic techniques such as GPS and Doppler orbitography and radiopositioning integrated by satellite (DORIS) will be critical to further reduce the error in the instrumental calibration.

With over a decade of precision sea level measurements from satellite altimetry in hand and with the recent launch of new satellite missions addressing different aspects of sea level rising, observationally, we have more information on sea level change than ever before. The latest globally averaged sea level change estimated from satellite altimeter (Fig. 10), 3.4 ± 0.4 mm/yr, is significantly larger than the historical rate of sea level change measured by tide gauges during the past decades (in the range of 1–2 mm/yr). This would imply a huge recent acceleration of sea level rise to get to the corrected rate of observed by altimetry. Moreover, satellite altimetry has given, for the first time, information about sea level change in open oceans and shown that sea level trends are not geographically uniform: some regions exhibiting trends about 10 times the

global mean [Cazenave and Nerem, 2004]. While the exact causes of the observed patterns are still unknown, such a result is crucial when considering coastal impacts of sea level rise, some regions being clearly much more vulnerable than others. However, a number of critical questions remain to be answered, particularly with regard to predicting the amount of sea level rise we will see in the next century. The rate inferred from altimeter could still be influenced by decadal variations of sea level unrelated to long-term climate change, such as the Pacific Decadal Oscillation. It is still unclear how much of the sea level rise shown in Fig.10 comes from long-term trend and how much from decadal variability. Thus, a longer time series is needed.

Low frequency sea level variability has also been a focus of research with the availability of long record altimetry data. For example, using 11 years measurements from T/P and Jason-1, Li and Clarke [2007] examined the interannual variability of sea level in the South Pacific from 5^{o}-28^{o}S. They found that in this region most of the interannual variability occurs west of 160^{o}W with root mean square value exceeding 11 cm; while east of 160^{o}W sea level variability is very low, less than 3 cm. Model simulation implied that the high sea level variability in the west is mainly due to the first and second baroclinic modes response to the interannual wind stress curl. The low-variability in the east can be attributed to the weak amplitude of sea level variability along the eastern coast; as a result, the Rossby wave source for the signal in the interior ocean is weak. Combining altimetry data and tide coastal gauge data, Clarke and Li [2004] and Li and Clarke [2004, 2005] also investigated the interannual coastal sea level variability and the associated geostrophic flows. They found that low-frequency currents exist along the coastal regions, such as western and southern Australian coast and the coast of Gulf of Mexico, and their existence is usually associated with large scale climate variability and strongly depends on the coastline direction and the mean background flows. Qiu and Chen [2006] have investigated the

decadal variability in the large-scale SSH field of the South Pacific using 12 year period of altimetry data. They found that the decadal SSH signals in the 1990s were dominated by an increasing trend in the 30°–50°S band and a decreasing trend in the central South Pacific Ocean poleward of 50°S. In recent years since 2002 there has been a reversal in both of these trends. Spatially varying low-frequency SSH signals are also found in the tropical region of 10°–25°S where the decadal SSH trend is negative in the eastern basin, but positive in the western basin. Qiu and Chen [2006] further investigated the underlying physics and found that accumulation of the wind-forced SSH anomalies along Rossby wave characteristics is important for both previously reported long-term trends and their reversals in recent years. The boundary forcing associated with the time-varying SSH signals along the South American coast is crucial for understanding the observed SSH signals of all time scales in the eastern tropical South Pacific basin, but it has little impact upon the midlatitude interior SSH signals.

8. MEANDERING JET

A surprise finding of the high-resolution multi-mission mapping is that zonal jets with the alternating east-west velocity populate every part of the world ocean and its marginal seas. This provides a unique opportunity for comprehensive study of the jets dynamics. These alternating jets are also observed in annual mean currents from model at 1000 m depth [Nakano and Hasumi 2005]. Using 18-week smoothed AVISO geostrophic velocity, Maximenko et al [2005] have shown that alternating jet-like structures are seen in the anomalous geostrophic velocity (Fig 11) and in every part of the global ocean. Their widths differ from place to place and generally decrease poleward. In some regions, the jets seem to be not exactly zonal. For instance, in the Gulf Stream extension (around 40^{o}N, 60^{o}W) they are systematically tilted from the west-southwest to the east-northeast. Mesoscale eddies are known to move westward [Cushman-

Roisin et al., 1990]. Theoretically, a typical individual eddy, when smoothed in time, would produce a zonally elongated structure with its width corresponding to the eddy size and its length defined by the displacement of the eddy. However, Maximenko et al [2005] argued that the length of the near zonal jet exceeds the estimated displacement of the eddy by a factor of 2–2.5 for the 18-week average.

In addition, using QuikSCAT wind stress and geostrophic currents from multi-mission satellite altimeter measurements from 2000 through 2006, Xu and Scott [2008a] have shown persistent small-scale features, which has never been seen in the previous studies, in the map of wind power input rate into World Ocean as shown in Fig 12. The wind power input field reveals narrow ribbons of both positive (red) and negative (blue) power input. Over most of the Southern Ocean the ribbons are woven together in a complex structure, but appear as organized zonal jets off the coast of Chile, extending up to half way to New Zealand. These fine features mainly arise from small-scale features of high-resolution merged altimeter data since wind field has a spatial scale larger than that of ocean field. It is surprising that alternating zonal jets dominate the fine structure of the map after five-year average. During this five-year period numerous oceanic eddies that have passed through the same area should have largely canceled the effects of each other. The fact that this is not happening may imply that paths of individual eddies are not completely random.

Godfrey [1989] has suggested that in regions where the ocean circulation can be considered to be in Sverdrup balance in the ocean interior, with the circulation closed by a western boundary current, the introduction of an island into the domain can result in the appearance of zonal jets reaching westwards from the northern and southern tips of the island. Using a global numerical ocean model, Hughes [2002] showed that the predicted zonal jets to the west of islands in and

near the Coral Sea in the southwest Pacific is seen in the merged (T/P and ERS) data. However, it cannot explain all the ubiquitous, patchy current structures in the World Ocean as seen by satellite altimetry. It is still unclear whether these structures are real jets or are propagating eddies smoothed in time. Further investigation of the mechanism of the zonal jets is still necessary.

9. CHALLENGES AND PERSPECTIVES

One main limitation of standard nadir-looking radar altimeters is spatial and temporal resolution, which is expected to be a limiting factor for the determination of mesoscale phenomena in deep ocean basins. Aliasing arises when high frequency signals are sampled infrequently and become indistinguishable from low frequency signals. High frequency signal varies greatly at different regions depending on their specific geographic [Xu et al. 2007, 2008; Stammer et al., 2000]. Since these signals cannot be resolved with any of the analyzed configurations and the sampling intervals vary among different altimeters, they strongly limit the mapping accuracy. Although multi-mission mapping technique has greatly improved the capability of altimetry to resolve mesoscale signal, Le Traon and Dibarbure [2002] reported that the high-wavenumber high-frequency signals contribute to the total velocity variance by up to 20% in high eddy energy regions. This explains why the velocity mapping errors remain larger than about 15%–20% of the signal variance even for the four satellite configurations. Most strikingly, Xu et al. [2008b] showed that combined spatio-temporal aliasing can produce unreal mesoscale signals in altimeter observations as shown in Fig 13, which changes the interpretation of the map significantly. The unreal mesocale signal (highlighted area in Fig 13) was produced by the combined aliasing from several neighboring and crossing tracks as explained in Xu et al [2008b]. Combined aliasing from a group of ground-tracks is a more obstinate aliasing problem

than ‘trackiness’ because of its extensive spatio-temporal influence. Altimeter missions were designed under the assumption that with the exception of a few special places (particularly near western boundary currents and near the equator), little difficulty would be experienced from the presence of energetic high frequency motions. The finding of the unreal mesoscale signal in the merged seal level anomaly product indeed casts a new challenge for future research.

Another major limitation of the altimetric system is related to the orbit determination quality, which is required to achieve the proper accuracy of the sea level determination in a geocentric reference frame. Altimetry measurement is performed from a spacecraft, which implies the use of global satellite tracking systems, such as Doris and/or GPS, and outstanding numerical orbit processing methods in order to reach an orbit determination accuracy compatible with the centimeter level precision of data. Although GRACE mission have greatly improved geoid estimate and has errors at length scales greater than 200krn at least 100 times smaller than the previous estimate such as EGM96 geoid, the GRACE geoid is much too smooth (signals with short wavelengths are missing). Thus, the geostrophic velocity derived from the anomalous SSH after removing the geoid shows spurious short-scale structures. Moreover, even for the perfect geoid, lateral uncertainty of altimeter tracks can introduce a notable extra error where the gradient of the geoid is large such as shelf break [Xu, 2006].

Despite above limitations, significant efforts have been made to improve altimetry measurement and promote its applications. A global barotropic model [Salto/Duacs User Handbook, 2006] has been used for high frequency (i.e less than 20 days) SSH signals correction. Xu et al. [2008b] has provided an effective way to de-alias of large-scale high-frequency barotropic signals from satellite altimetry with bottom pressure measurements in

marginal seas. At the mean time, various exciting technology and research programs have been proposed for future satellite altimetry development.

Future altimeter concepts mainly address the issues of improving sampling and improving data provision through a wider range of parameters, or improvement of the reliability/accuracy of the currently available parameters. Future altimeter concepts include constellation of micro-satellite altimeters – Altika and GANDER [Jolly and Allan, 2000], Wittex [Raney and Porter, 2001], SWIMSAT [Hauser, 2001], and Wide Swath Altimetry. Wide Swath Ocean Altimeter (WSOA) proposed by Fu [2003] was designed to be flown with Jason-1 class conventional dual-frequency altimeter system, including a multi-frequency radiometer for the correction of the effects of water vapor in the troposphere. WSOA will extend the measurement from a line along the nadir to a swath of 200 km centered on the nadir track. The most important application of WSOA is to provide the first synoptic maps of the global oceanic eddy field. The swath measurement of WSOA system is based on the concept of radar interferometry described in Fig 14. The instrument consists of two side-looking fan-beam antennae separated by a boom with a length of 5-10 m. WSOA measures the relative delay between the ocean-reflected signals from two antennas separated by a "baseline distance". The range measurements from the two antennas and the baseline form a triangle that can be used to determine the location of the target in the observation plane. The measurement triangle is made up of the baseline B, and the ranges from the target to the two antennas, r1 and r2. The range r1 is determined by system timing measurements. The incidence angle θ can be obtained from the range difference Δr. Given these measurements, the height h above a reference plane can be obtained using the equation $h = H - r_1 \cos(\theta)$, where H is the altitude of the satellite determined from orbit ephemeris. The strong currents and water property anomalies (in temperature, salinity, oxygen, etc.) associated

with ocean eddies are a major factor affecting the oceanic general circulation and maritime operations such as offshore oil drilling, ship routing, fisheries, marine debris dispersion, etc. WSOA is expected to be an essential part of the future ocean observing system for addressing these applications.

The performance of satellite borne radar altimeters has probably contributed more to our understanding of global ocean process than any other single satellite sensor. The combination of high-resolution altimetry and other captors or in-situ data is also a field full of possibilities. Combining altimeter observations and ocean color measurements can give us enormous insight into the biological coupling associated with mesoscale eddies and fronts. Satellite altimetry and Argo float are two essential components of the global ocean observing system. They are strongly complementary. Altimetry provides global, real time, all-weather sea level measurements with high space/time resolution. Whereas Argo float gives the global temperature and salinity vertical distribution. Altimeter and Argo data can be jointly used in most ocean hindcasting, nowcasting and forecasting models. Altimeter data can be used to develop operational oceanography services (e.g. safe and efficient offshore activities, pollution monitoring, environmental management, security and sustainable use of marine resources) for ocean, environment, and climate research since most operational oceanography applications require high resolution surface currents that cannot be adequately reproduced without a high resolution altimeter system (e.g. Fig 15). The critical issue is now to ensure a long-term commitment for an operational high resolution altimeter system which is needed both for research and operational applications, especially in the coastal domain (e.g. marine security and pollution monitoring that require high resolution surface currents).

Figure captions:

Figure 1 (a) T/P and (b) T/P + ERS-1/2 rms SLA variability. Maps from October 1992 to December 1993 and from March 1995 to October 1997 are used (time gap is the missing ERS-1 period). Units are centimeters. Adapted from Ducet et al. (2000)

Figure 2 Sea level anomaly maps over the Mediterranean for 11 June 2003, from Jason-1 + ERS-2 (top) and Jason-1+ERS-2+T/P+GFO (bottom). Merging the data from the four satellites shows eddies (circles) that are invisible, or barely visible with two satellites are much better resolved with four. (Credits MFS/CLS)

Figure 3. EKE, in $cm^2\ s^{-2}$, inferred from the 5 year period of (a) zonal and (b) meridional components of the geostrophic velocity variance from Ducet et al (2000).

Figure 4 The eddy characteristics in 1^o squares for eddies with lifetimes > 4 weeks: (a) The number of eddies of both polarities (white areas correspond to no observed eddies); (b) the mean amplitude; (c) the mean diameter; and (d) the percentage of SSH variance explained (white areas correspond to 0%). The contour in each panel is the 4 cm standard deviation of filtered SSH. Adopted from Chelton et al. (2007)

Figure 5 Mean tidal energy fluxes of the M_2 barotropic tide, determined from 6-year T/P altimeter measurements. (Credit Richard Ray, NASA GSFC)

Figure 6 Mean tidal energy fluxes of the temporally coherent M_2 internal tide, averaged over ocean bins of size 4 x 3 degrees (Ray and Cartwright, 2001). Flux vectors smaller than 100 W/m are not shown. Bathymetry contours are given every 1000 m.

Figure 7 Sea surface height from T/P during the period (a) El Niño and (b) La Niña
(Credit DUACS)

Figure 8 Planetary waves from T/P measurements.

Figure 9 T/P tide gauge calibration values from Mitchum [2000] used to diagnose changes in the altimeter calibration. These values represent 10-day global averages of T/P minus tide gauge sea level differences using T/P data in the vicinity of 64 different tide gauges

Figure 10 Global mean sea level change from T/P and Jason measurements (effects of glacial isostatic adjustment is not included). Concurrent tide gauge calibrations (1998, 2000) are used to estimate altimeter drift. (Credit University of Colorado)

Figure 11 Anomaly of AVISO altimeter zonal geostrophic velocity averaged over 18 weeks from Maximenko et al. (2005).

Figure 12 Wind power input to the surface geostrophic current from satellite measurements averaged over a period from 2000 to 2005 (right panel, in units of $mW\ m^{-2}$), and the meridional

distribution of the zonal integral (left panel). Persistent small scale features in the wind stress and ocean surface current are clearly seen. Adopted from Xu et al. (2008a)

Figure 13 Sea level anomaly from the AVISO merged (T/P+ERS2) product. The circled area is produced by the aliasing error from the combined aliasing from several neighboring and crossing tracks from Xu et al. (2008b).

Figure 14 Geometric concept used for radar interferometry (Credit AVISO).

Figure 15 Operational oceanography applications: Marine Pollution (Prestige). The real time description and forecast of surface currents is not possible without a high resolution altimeter system (credit Pierre-Yves Le Traon)

Reference

Aristegui J. P, S. Sangra., Hernandez-Leon, M. A. Canton., Hernandez-Guerra, and J. L. Kerling, 1994: Islands-induced eddies in the Canary Islands, Deep Sea Res., 41, 1509-1525.

Brandt, P., F. A. Schott, A. Funk, and C. S. Martins, 2004: Seasonal to interannual variability of the eddy field in the Labrador Sea from satellite altimetry, J. Geophys. Res., 109, C02028, doi:10.1029/2002JC001551.

Cazenave, A., and R. S. Nerem, 2004, Present-day sea level change: Observations and causes, Rev. Geophys., 42, RG3001, doi:10.1029/2003RG000139.

Chambers, D., J. Ries, C. Shum, and B. Tapley, 1998, On the use of tide gauges to determine altimeter drift, J. Geophys. Res., 103(C6), 12885-12890

Chelton, D. B., and Schlax, M. G., 1996: Global observations of oceanic Rossby waves, Science, 272, 234-238.

Chelton, D. B., and M. G. Schlax, 2003: The accuracies of smoothed sea surface height fields constructed from tandem altimeter datasets, J. Atmos. Oceanic Technol., 20, 1276– 1302.

Chelton, D. B., M. G. Schlax, R. M. Samelson, and R. A. de Szoeke, 2007: Global observations of large oceanic eddies, Geophys. Res. Lett., 34, L15606, doi:10.1029/2007GL030812.

Clarke, A. J., and J. Li, 2004: El Niño/La Niña shelf edge flow and Australian western lobsters. Geophys. Res. Lett., 31, L11301, doi: 10.1029/2003GL018900

Cummins, P. F., G. S. E. Lagerloef, and G. Mitchum, 2005, A regional index of northeast Pacific variability based on satellite altimeter data, Geophys. Res. Lett., 32, L17607, doi:10.1029/2005GL023642

Cushman-Roisin, B., E. P. Chassignet, and B. Tang, 1990, Westward motion of mesoscale eddies, J. Phys. Oceanogr., 20, 97–113.

Dewar, W.K., 1998: On “too-fast” baroclinic planetary waves in the general circulation. J. Phys. Oceanogr., 28, 1739-1758.

Dong, S., and K.A. Kelly, 2004: Heat Budget in the Gulf Stream Region: The Importance of Heat Storage and Advection. J. Phys. Oceanogr., 34, 1214–1231.

Dong, S., 2004, Interannual Variations in Upper Ocean Heat Con- tent, Heat Transport, and Convergence in the Western North Atlantic, Ph. D. thesis, School of Oceanography, University of Washington.

Douglas, B. C., and R. E. Cheney, 1990: Geosat: Beginning a new era in satellite oceanography. J. Geophys. Res, 95, 2833-2836.

Ducet, N., Le Traon, P.Y., Reverdin, G., 2000. Global high resolution mapping of ocean circulation from the combination of TOPEX/ POSEIDON and ERS-1/2. J. Geophys. Res. 105 (C8), 19477–19498.

Egbert,G . D., and R. D. Ray, Significant tidal dissipation in the deep ocean inferred from satellite altimeter data, Nature, 405, 775-778, 2000.

Frankignoul C., and P. Müller, 1979: Quasi-geostrophic response of an infinite β -plane ocean to stochastic forcing by the atmosphere. J. Phys. Oceanogr. 9, 104-127.

Fu, L.-L., 1983: Recent progress in the application of satellite altimetry to observing the mesoscale variability and general circulation of the oceans. Rev. Geophys. Space. Phys. 21, 1657-1666.

Fu. L.L., E. J. Christensen, C. A. Yamarone Jr., M. Lefebvre, Y. Menard, M. Dorrer, and P. Escudier, 1994: TOPEX/POSEIDON mission overview. J. Geophys. Res., 99, 24 369–24 381.

Fu, L.-L, and R. E. Cheney, 1995: Application of satellite altimetry to ocean circulation studies: 1897-1994. Rev. Geophys., 32, Supplement, 213-223.

Fu, L.-L. and D.B. Chelton, 2001. Large-scale ocean circulation. In, Satellite Altimetry and Earth Sciences. A Handbook of Techniques and Applications, Academic Press ed. L.-L. Fu and A. Cazenave, Eds., Academic Press, 133-169.

Fu, L.-L. editor, 2003: Wide-Swath Altimetric Measurement of Ocean Surface Topography. *JPL Publication 03-002*. Jet Propulsion Laboratory, Pasadena, CA. 67 pp

Fu, L.-L., D. Stammer, B. B. Leben, and D. B. Chelton, 2003: Improved spatial resolution of ocean surface topography from the TOPEX/Poseidon—Jason-1 tandem altimeter mission, Eos Trans. AGU, 84(26), 241, 247– 248.

Godfrey, J. S., 1989, A Sverdrup model of the depth-integrated flow for the world, allowing for island circulations, Geophys. Astrophys. Fluid Dynamics, 45, 89– 112.

Gille, S.T., 1994. Mean sea surface height of the Antarctic Circumpolar Current from GEOSAT data: methods and application. J. Geophys. Res., 99, 18255-18273.

Greenslade, D.J.M., D.B. Chelton and M.G. Schlax, 1997, The Midlatitude resolution capability of sea level fields constructed from single and multiple satellite altimeter datasets, *J. Atm. Ocean. Tech*., **14**, 849 -870.

Hauser R D., SWIMSAT - Surface Waves Investigation and monitoring from Satellite, A proposal to the Earth Explorer Opportunity Missions of ESA., 2001.

Heywood, K. J., D. P. Stevens, and G. R. Bigg, 1996: Eddy formation behind the tropical island of Aldabra. Deep-Sea Res, 43, 555-578.

Holland, C. L., and G.T. Mitchum, 2001: Propagation of Big Island Eddies. J. Geophys. Res., 106, 935-944.

Hughes, C.W., 2002, Zonal jets in and near the Coral Sea, seen by satellite altimetry, Geophys. Res. Lett., 29(9), 1330, doi:10.1029/2001GL014006

Isern-Fontanet, J., E. Garcia-Ladona, and J. Font, 2003: Identification of marine eddies from altimetric maps, J. Atmos. Oceanic Technol., 20, 772– 778.

Isern-Fontanet, J., E. Garcia-Ladona, and J. Font, 2006: Vortices of the Mediterranean Sea: An altimetric perspective, J. Phys. Oceanogr., 36, 87– 103.

Jayne, S.R. and J. Marotzke, 2002, The oceanic eddy heat transport. J. Phys. Oceanogr., 2, pp. 3328–3345

Jolly, GW, and Allan, T.D, GANDER Technical Feasibility Study, Report to the British National Space Centre, November 2000.

Joyce, T.M., K.A. Kelly, D.M. Schubert and M.J. Caruso, Shipboard and Altimetric Studies of Rapid Gulf Stream Variability Between Cape Cod and Bermuda, *Deep-Sea Res., 37,* 897--910, 1990.

Karsten, R.H. and J. Marshall, 2002. Constructing the Residual Circulation of the ACC from Observations. J. Phys. Oceanogr., 32, 3315–33,277.

Kelly, K.A. and S.T. Gille, Gulf Stream Surface Transport and Statistics at 69^{o} W from the Geosat Altimeter, *J. Geophys. Res., 95(C3),* 3149--3162, 1990.

Kelly, K. A., The relationship between oceanic heat trans- port and surface fluxes in the western North Pacific: 1970-2000, J. Clim., 17, 573-588, 2004.

Killworth, P. D., D. B. Chelton, and R. A. De Szoeke, 1997, The speed of observed and theoretical long extra-tropical planetary waves, J. Phys. Oceanogr., 27, 1946-1966.

Killworth, P. D., and J.R. Blundell, 2003, Long Extratropical Planetary Wave Propagation in the Presence of Slowly Varying Mean Flow and Bottom Topography. Part I: The Local Problem. *J. Phys. Oceanogr.*, 33, 784–801.

Le Traon, P. Y., 1992: Contribution of satellite altimetry to the observation of oceanic mesoscale variability. Oceanologica Acta, 15, 441-457.

Le Traon, P. Y., and F. Ogor, 1998: ERS-1/2 orbit improvement using TOPEX/Poseidon: the 2 cm challenge. J. Geophys. Res., 95, 8,045-8057.

Le Traon, P.-Y., P. Gaspar,F . Ogor, and J. Dorandeu, Satellites work in tandem to improve accuracy of data, Eos Trans. AGU, 76, 385- 389, 1995.

Le Traon P.Y., F. Nadal and N. Ducet, 1997. An improved mapping method of multi-

Le Traon, P.-Y., and F. Ogor, ERS-1/2 orbit improvement using TOPEX/Poseidon: The 2 cm challenge J, . Geophys R. es.,1 03, 8045- 8057, 1998.

Le Traon, and G. Dibarboure, 1999: Mesoscale mapping capabilities from multiple altimeter missions. J. Atmos. Oceanic Technol., 16, 1208–1223.

Le Traon, P.Y. and G. Dibarboure, 2002, Velocity mapping capabilities of present and future altimeter missions: the role of high frequency signals. *J. Atm. Ocean Tech.,* **19**, 2077-2088.

Le Traon, P.-Y. and R. A. Morrow, 2001, Ocean currents and mesoscale eddies. Satellite Altimetry and Earth sciences. A Handbook of Techniques and Applications, Academic Press ed. L.-L. Fu and A. Cazenave, Eds., Academic Press, 171-215.

Li, J., and A. J. Clarke, 2004, Coastline direction, interannual flow, and the strong El Niño currents along Australia's nearly zonal southern coast. J. Phys. Oceanogr., 34, 2373-2381.

Li, J., and A. J. Clarke, 2005, Interannual flow along the northern coast of Gulf of Mexico. J. Geophys. Res. Vol.110,C11002,doi:10.1029/2004JC002606.

Li, J., and A. J. Clarke, 2007, Interannual sea level variations in the South Pacific from 5^{o} to 28^{o}S. J. Phys. Oceanogr., 37, 2882-2894.

Maximenko, N. A., B. Bang, and H. Sasaki, 2005, Observational evidence of alternating zonal jets in the World Ocean, Geophys. Res. Lett., 32, doi:10.1029/2005GL022728.

Mitchum, G.T., 1994, Comparison of TOPEX sea surface heights and tide gauge sea levels. J. Geophys. Res., 99, 24,541-24,553

Mitchum, G.T., 1997, Altimeter Drift from Tide Gauges. AVISO Altimetry Newsletter, Number 5, 8-11

Mitchum, G. T., 1998: Monitoring the Stability of Satellite Altimeters with Tide Gauges, Journal of Atmospheric and Oceanic Technology, 15(3), 721-730.

Mitchum, G. T., 2000, An Improved Calibration of Satellite Altimetric Heights Using Tide Gauge Sea Levels with Adjustment for Land Motion, *Marine Geodesy*, 23(3), 145-166.

Morrow, R., F. Birol, D. Griffin, and J. Sudre, 2004: Divergent pathways of cyclonic and anti-cyclonic ocean eddies, Geophys. Res. Lett., 31, L24311, doi:10.1029/2004GL020974.

Müller, P., and C. Frankignoul, 1981: Direct atmospheric forcing of geostrophic eddies. J. Phys. Oceanogr., 11, 287-308.

Nakano, H. and H. Hasumi, 2005. A series of zonal jets embedded in the broad zonal flows in the Pacific obtained in eddy-permitting ocean general circulation models. J. Phys. Oceagr., 35(4), 474-488.

Pascual A., M.I. Pujol, G. Larnicol, P.Y. Le Traon and M.H. Rio, 2007. Mesoscale mapping Capabilities of Multisatellite Altimeter Missions: First Results with Real data in the Mediterranean Sea. J. Mar. Systems, 65, 190–211.

Pascual, A., Y. Fauge`re, G. Larnicol, and P.-Y. Le Traon, 2006: Improved description of the ocean mesoscale variability by combining four satellite altimeters, Geophys. Res. Lett., 33, L02611, doi:10.1029/2005GL024633

Qiu, B., 1992, Recirculation and seasonal change of the Kuroshio from altimetry observations, J. Geophys. Res. 97, 17,801- 17,813.

Qiu, B., 2000, Interannual variability of the Kuroshio Exten- sion system and its impact on the wintertime SST field, J. Phys. Oceanogr., 30, 1486-1502.

Qiu, B., and S. Chen, 2005: Eddy-Induced Heat Transport in the Subtropical North Pacific from Argo, TMI, and Altimetry Measurements. J. Phys. Oceanogr., 35, 458-473.

Qiu, B., and S. Chen, 2006: Decadal variability in the large-scale sea surface height field of the South Pacific Ocean: Observations and Causes. J. Phys. Oceanogr., 36, 1751-1762.

Raney, R. K., and D. L. Porter, WITTEX: An innovative multi-satellite radar altimeter constellation, from “Report of the high resolution ocean topography science working group meeting”, ed D. Chelton. University of Maryland, 28-29 March 2001.

Ray, R. D., and D. E. Cartwright, 2001, Estimates of Internal Tide Energy Fluxes from Topex/Poseidon Altimetry: Central North Pacific, Geophys. Res. Lett., 28(7), 1259–1262.

Ray, R., and G.T. Mitchum, Surface manifestation of internal tides generated near Hawaii, Geophys. Res. Lttrs., 23, 2101-2104.

Ray, R., and G.T. Mitchum, Surface manifestation of internal tides in the deep ocean: Observations from altimetry and island gauges. Prog. Oceanogr., 40,135-162.

Richardson, P. L., 1983: Eddy kinetic energy in the North Atlantic from surface drifters. J. Geophys. Res., 88, 4355-4367.

Roemmich, D., and J. Gilson, 2001: Eddy transport of heat and thermocline waters in the North Pacific: A key to interannual/decadal climate variability?, J. Phys. Oceanogr., 31, 675–687.

Schmitz, W. J., Jr., and J. R. Luyten, 1991: Spectral time scales for mid-latitude eddies. J. Mar. Res. 49, 75-105.

Scott, R. B., and F. Wang, 2005: Direct evidence of an oceanic inverse kinetic energy cascade from satellite altimetry, J. Phys. Oceanogr., 35, 1650– 1666.

Scott, R. B., Y. Xu, 2008, An update on the wind power input to the surface geostrophic flow of the World Ocean, Deep-Sea Res. I, Under Review.

Ssalto/Duacs User Handbook, 2006, (M)SLA and (M)ADT Near-Real Time and Delayed Time Products, *SALP-MU-P-EA-21065-CLS*, Edition 1.5

Stammer, D., 1997: Global characteristics of ocean variability estimated from regional TOPEX/Poseidon altimeter measurements. J. Phys. Oceanogr., 27, 1743-1769.

Stammer, D., 1998: On eddy characteristics, eddy transports, and mean flow properties. J. Phys. Oceanogr., 28, 727-739.

Stammer, D., and C. Wunsch, 1999: Temporal changes in eddy energy of the oceans. Deep Sea Res. 46, 77-108.

Stammer, D., C. Wunsch, and R. M. Ponte (2000), De-aliasing of global high frequency barotropic motions in altimeter observations, Geophys. Res. Lett., 27, 1175–1178.

Stewart, R.H., Methods of Satellite Oceanography, 360 pp., University of California Press, Berkeley, CA, 1985.

Tai, C.K., Estimating the Basin-Scale Circulation from Satellite Altimetry. Part 1 : Straightforward Spherical Harmonic Expansion, *J. Phys. Oceanogr., 18(10),* 1398--1413, 1988.

Tai, C.K., 1998. On the spectral ranges that are resolved by a single satellite in exact- repeat sampling configuration. *J. Atmos. Ocean. Technol.*, **15**, 1459-1470

Traon, P.Y.L., and G. Dibarboure, 2002, Velocity Mapping Capabilities of Present and Future Altimeter Missions: The Role of High-Frequency Signals. J. Atmos. Oceanic Technol., 19, 2077–2087

Vivier, F., K. A. Kelly, and L. Thompson, 2002, Heat bud get of the Kuroshio Extension region: 1993-1999, J. Phys. Oceanogr., 32, 3436-3454.

Wunsch, C. and E.M. Gaposchkin, On Using Satellite Altimetry to Determine the General Circulation of the Oceans with Application to Geoid Improvement, *Rev. Geophys. Space Phys., 18(4),* 725--745, 1980.

Wunsch. C., Comment on R . N. Stewart's "Physical Oceanography to the end of the twentieth century" in Quo Vadirnus: Geophysics for the Next Generation, Geophys Monogr. Ser., vol. 60., edited by G.D. Garland and J. Apel, p.69, AGU, Washington, D.C., 1990.

Wunsch, C., Observing ocean circulation from space, *Oceanus, 35 (2),* 9--17, 1992.

Xu, Y., 2006, Analyses of sea surface height, bottom pressure and acoustic travel time in the Japan/East Sea, Ph.D. thesis, 86pp, Univ. of Rhode Island, Rohde Island, 26 September.

Xu, Y., D. R. Watts, M. Wimbush, and J.-H. Park, 2007, Fundamental-mode basin oscillations in the Japan/East Sea, *Geophys. Res. Lett.,* **34**, L04605, doi: 10.1029/2006GL028755

Xu, Y., R. B Scott , 2008a, Subtleties in forcing eddy resolving ocean models with satellite wind data, Ocean Modeling, 20, 240–251, doi:10.1016/j.ocemod.2007.09.003.

Xu, Y., D. R. Watts, and J.-H. Park, 2008b, De-aliasing of basin-scale high-frequency barotropic signals from satellite altimetry in the Japan/East Sea, J. Atmos. Oceanic Technol., In Press, doi: 10.1175/2008JTECHO582.1

Reviewed by

1. Alejandro H. Orsi
   Department of Oceanography, Texas A&M University, College Station, TX 77843-3146

2. Marcelo Dottori
   LOCEAN – IPSL, Université Pierre et Marie Curie aile 45-55 4ème étage Case 100 - 4 Place Jussieu 75252 Paris cedex 05

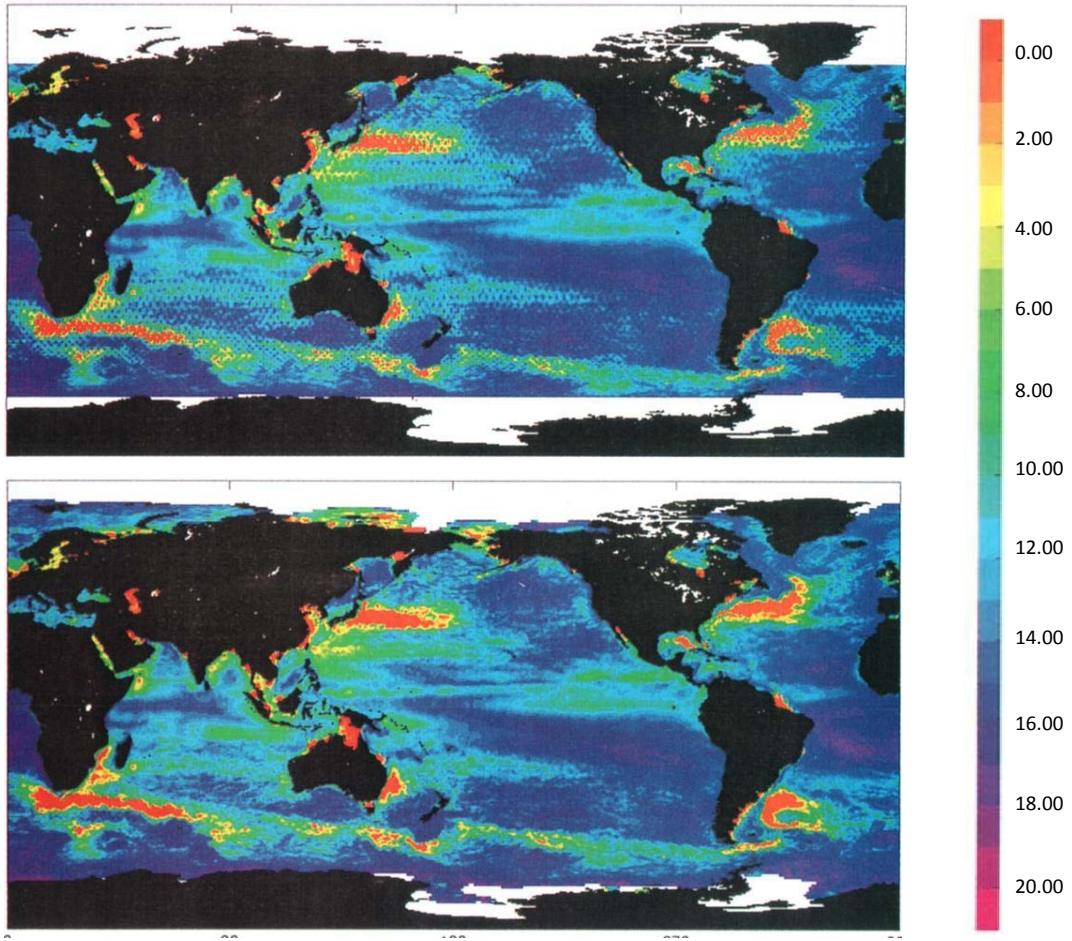

Figure 1. (a) T/P and (b) T/P + ERS-1/2 rms SLA variability. Maps from October1992 to December 1993 and from March 1995 to October 1997 are used (time gap is the missing ERS-1 period). Units are centimeters. Adapted from Ducet et al. (2000)

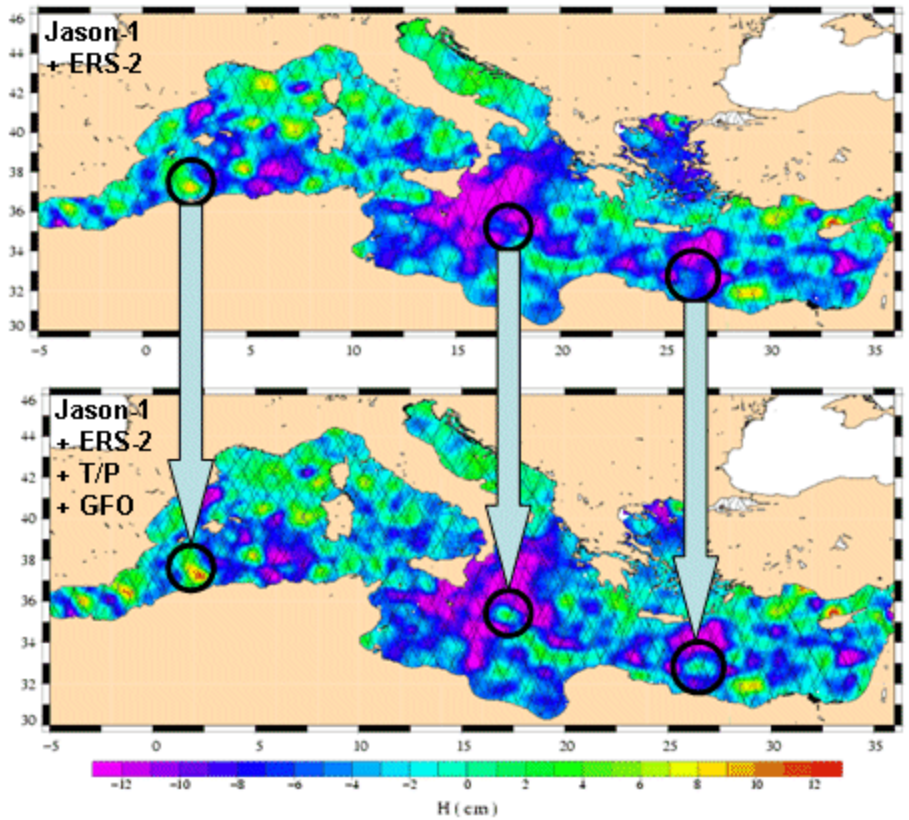

Figure 2. Sea level anomaly maps over the Mediterranean for11 June 2003, from Jason-1 + ERS-2 (top) and Jason-1+ERS-2+T/P+GFO (bottom). Merging the data from the four satellites shows eddies (circles) that are invisible, or barely visible with two satellites are much better resolved with four. (Credits MFS/CLS)

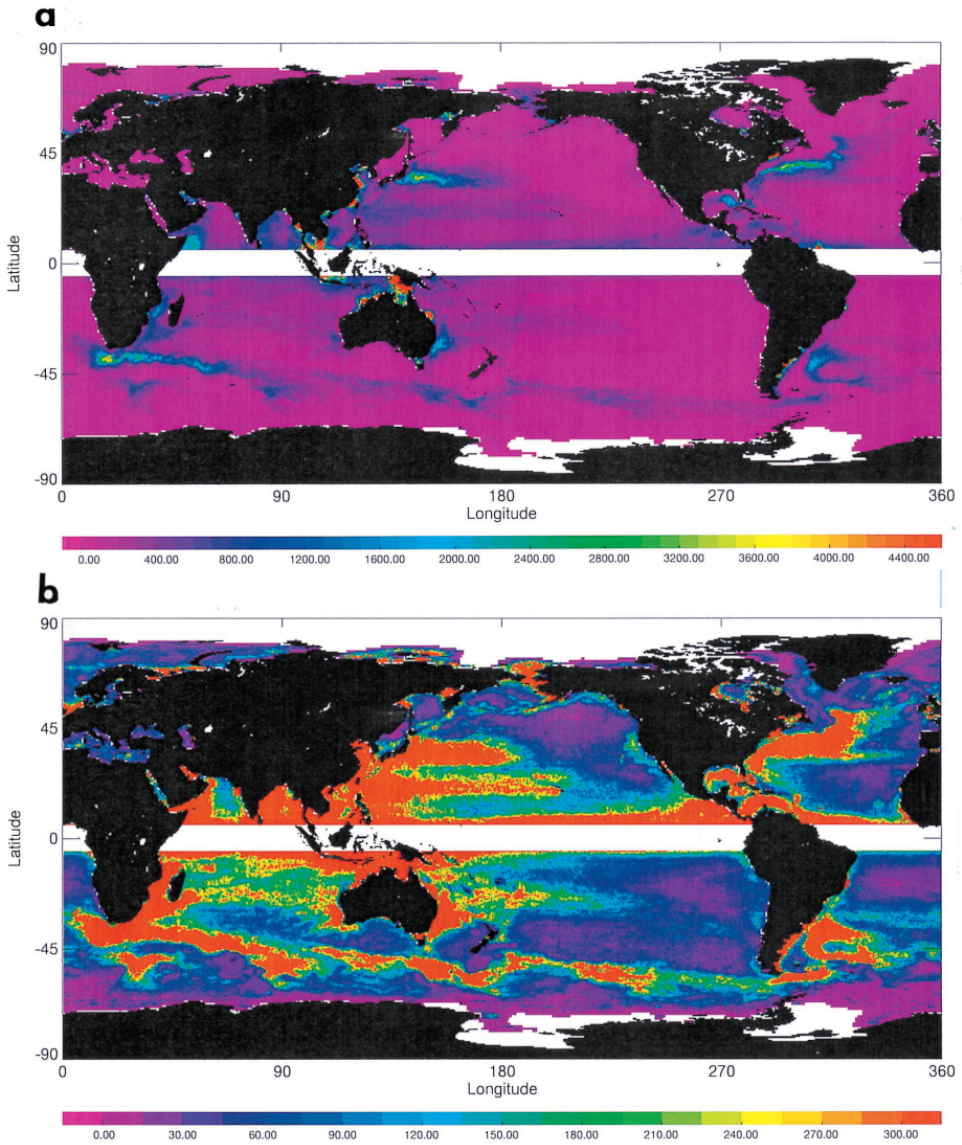

Figure 3. EKE, in $cm^2\ s^{-2}$, inferred from the 5 year period of (a) zonal and (b) meridional components of the geostrophic velocity variance from Ducet et al (2000).

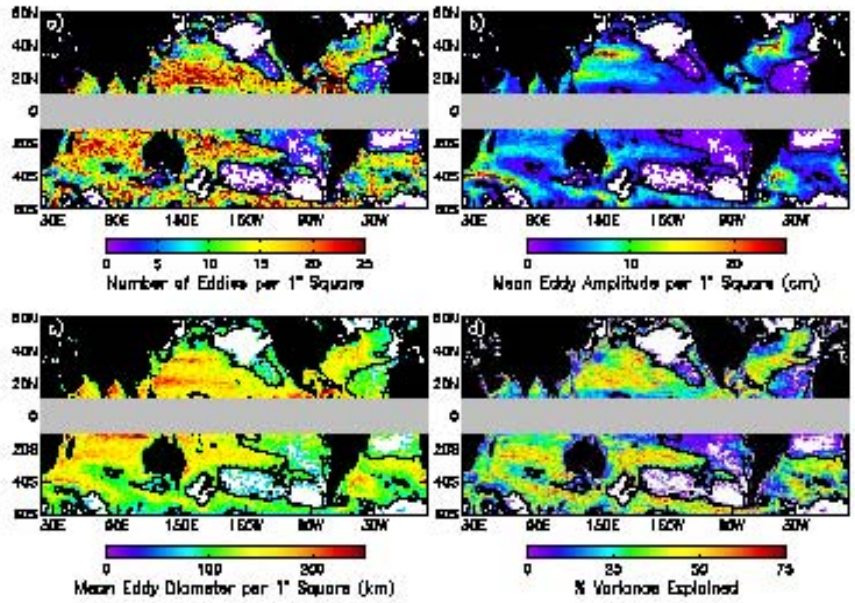

Figure 4 The eddy characteristics in 1° squares for eddies with lifetimes ≥ 4 weeks: (a) The number of eddies of both polarities (white areas correspond to no observed eddies); (b) the mean amplitude; (c) the mean diameter; and (d) the percentage of SSH variance explained (white areas correspond to 0%). The contour in each panel is the 4 cm standard deviation of filtered SSH. Adopted from Chelton et al. (2007)

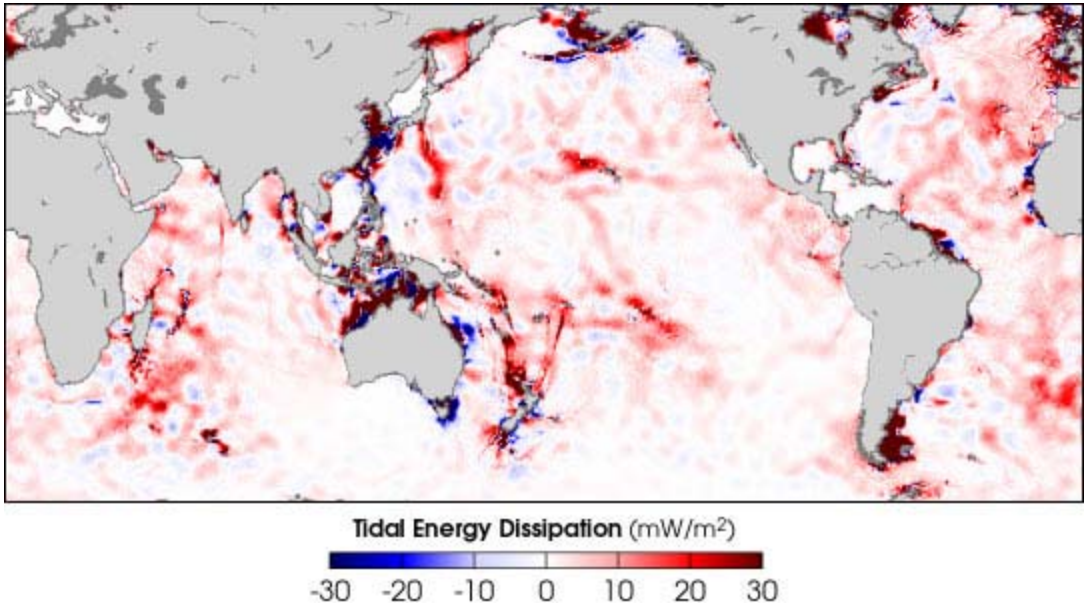

Figure 5. Mean tidal energy fluxes of the M_2 barotropic tide, determined from 6-year T/P altimeter measurements. (Credit Richard Ray, NASA GSFC)

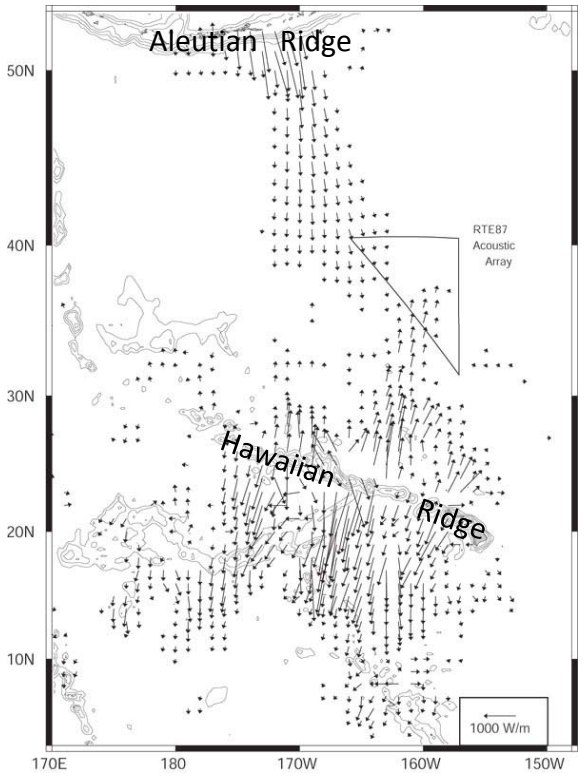

Figure 6. Mean tidal energy fluxes of the temporally coherent M_2 internal tide, averaged over ocean bins of size 4 x 3 degrees (Ray and Cartwright, 2001). Flux vectors smaller than 100 W/m are not shown. Bathymetry contours are given every 1000 m.

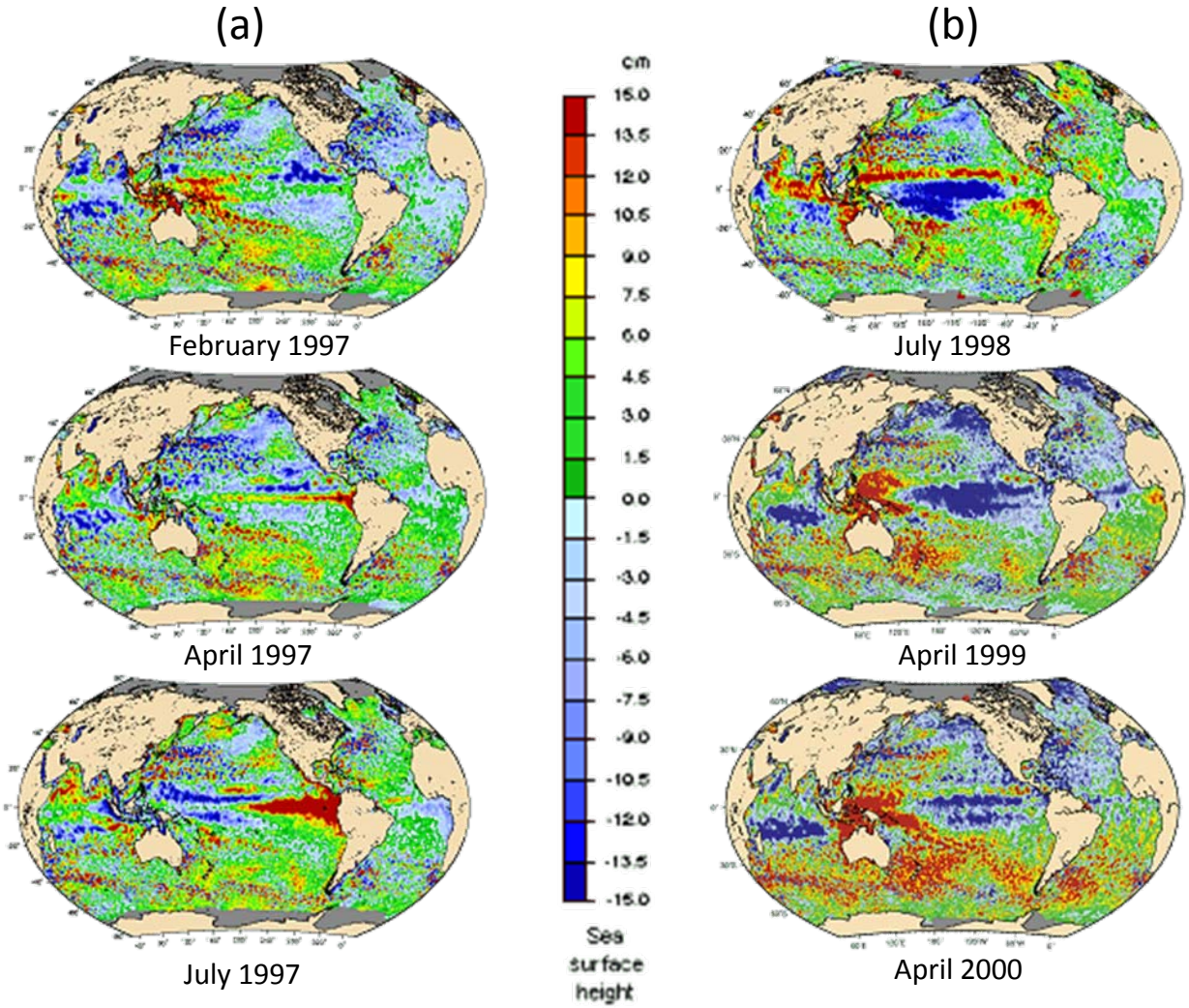

Figure 7. Sea surface height from T/P during the period (a) El Niño and (b) La Niña (Credit DUACS)

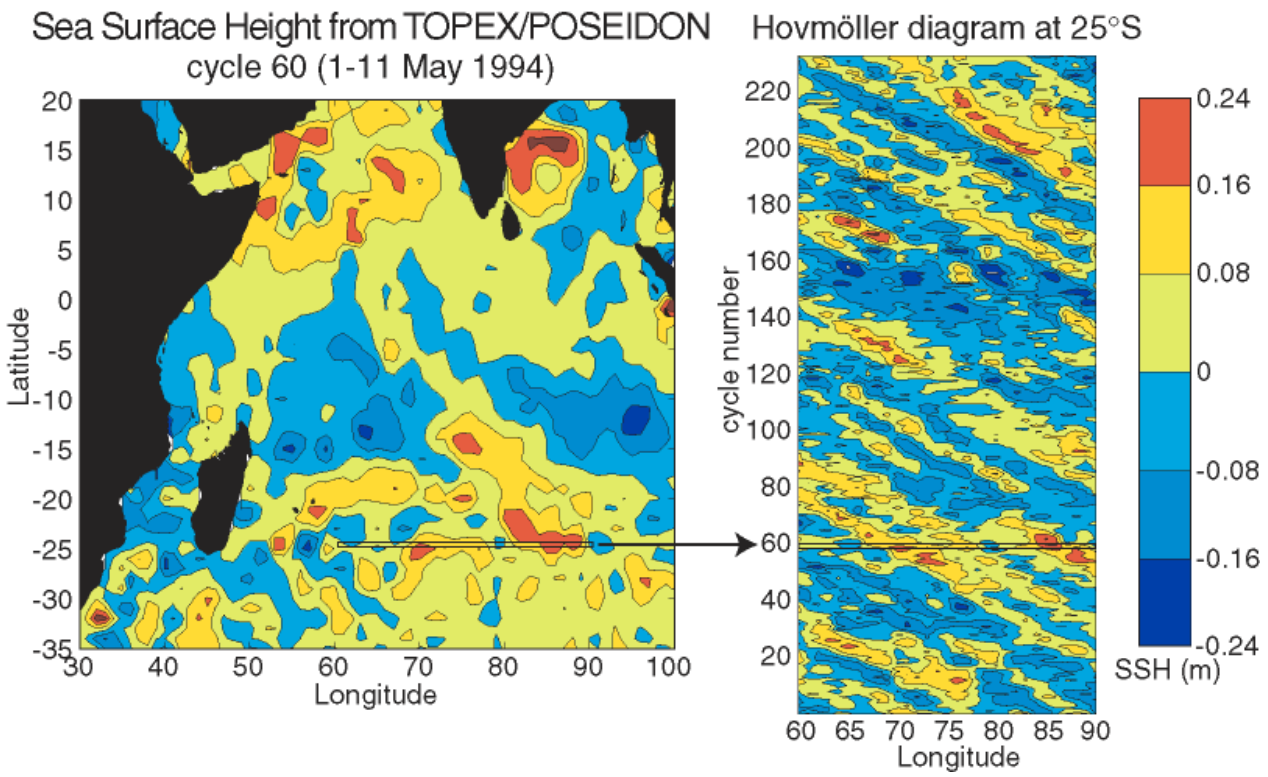

Figure 8. Planetary waves from T/P measurements.

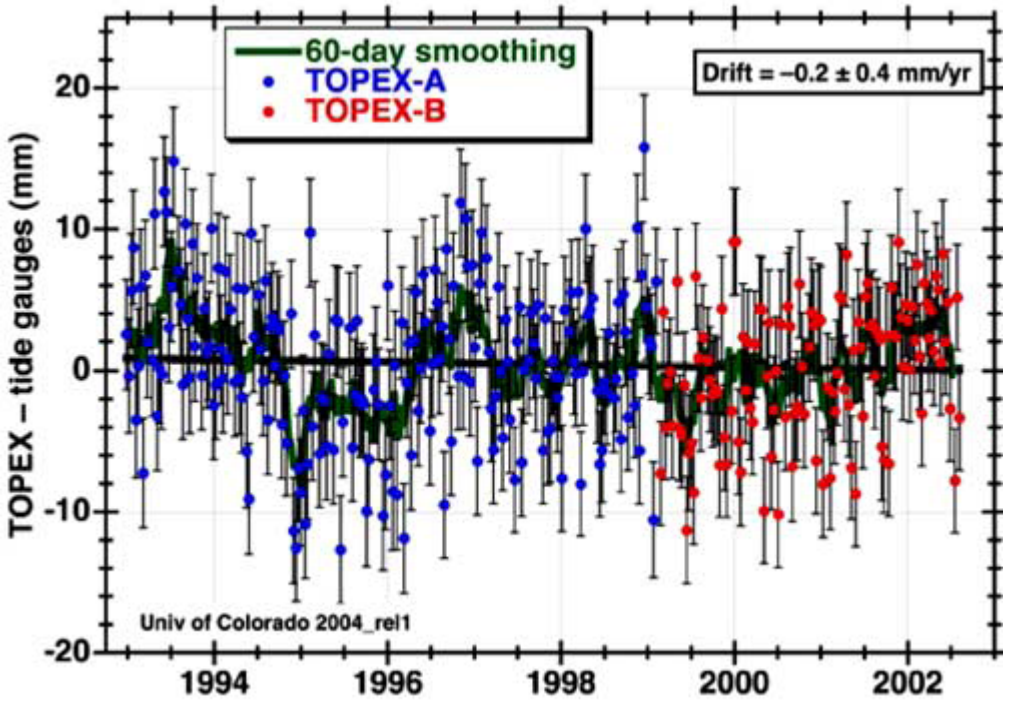

Figure 9. T/P tide gauge calibration values from Mitchum [2000] used to diagnose changes in the altimeter calibration. These values represent 10-day global averages of T/P minus tide gauge sea level differences using T/P data in the vicinity of 64 different tide gauges

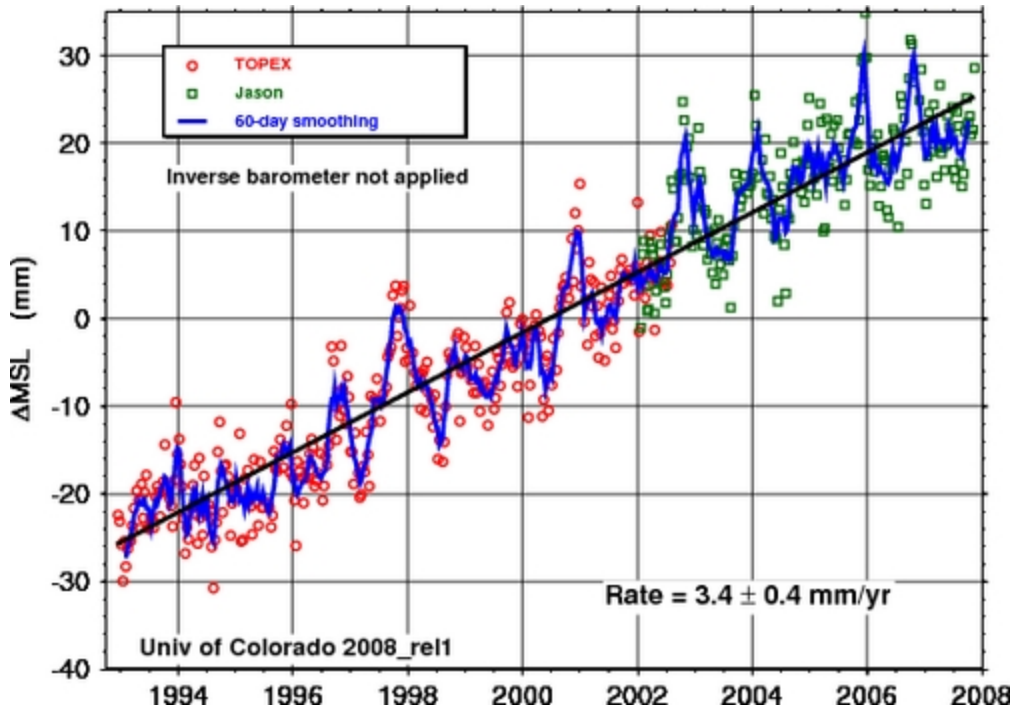

Figure 10. Global mean sea level change from T/P and Jason measurements (effects of glacial isostatic adjustment is not included) Concurrent tide gauge calibrations (1998, 2000) are used to estimate altimeter drift. (Credit University of Colorado)

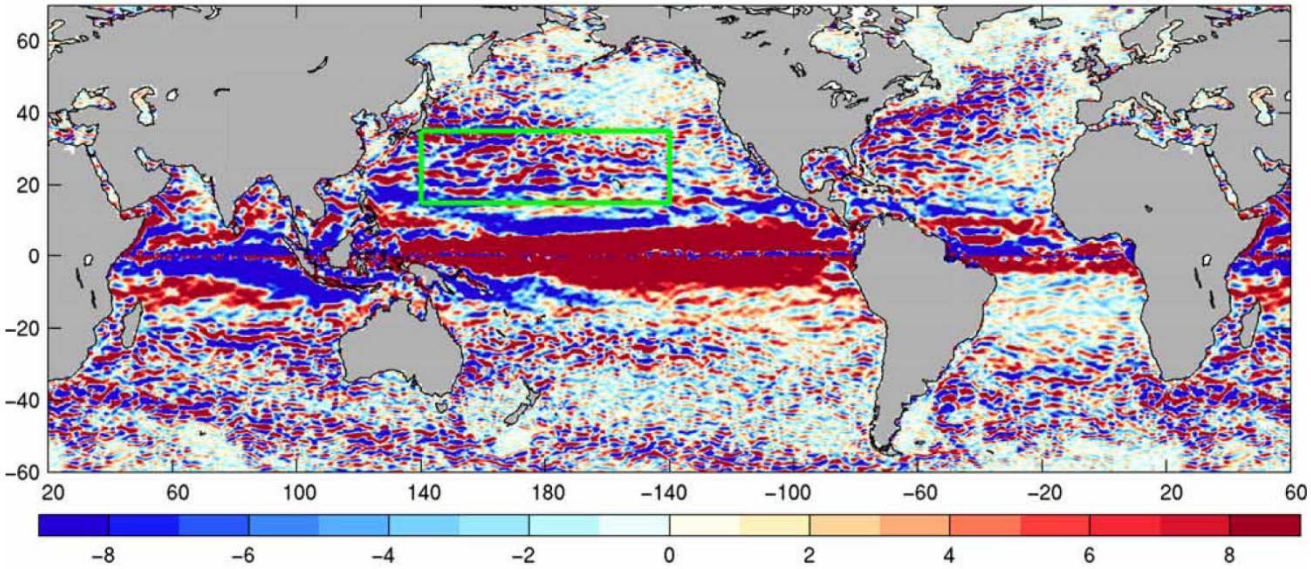

Figure 11 Anomaly of AVISO altimeter zonal geostrophic velocity averaged over 18 weeks from Maximenko et al. (2005).

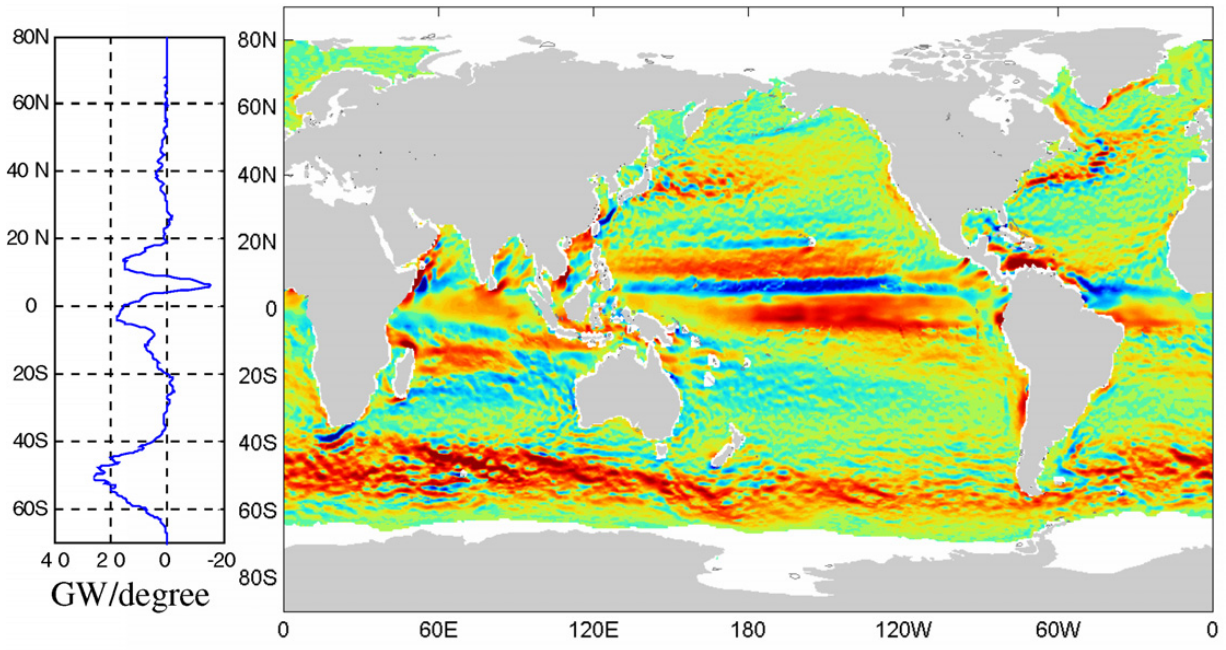

Figure 12 Wind power input to the surface geostrophic current from satellite measurements averaged over a period from 2000 to 2006 (right panel, in units of mW m^{-2}), and the meridional distribution of the zonal integral (left panel). Persistent small scale features in the wind stress and ocean surface current are clearly seen. Adopted from Xu et al. (2008a)

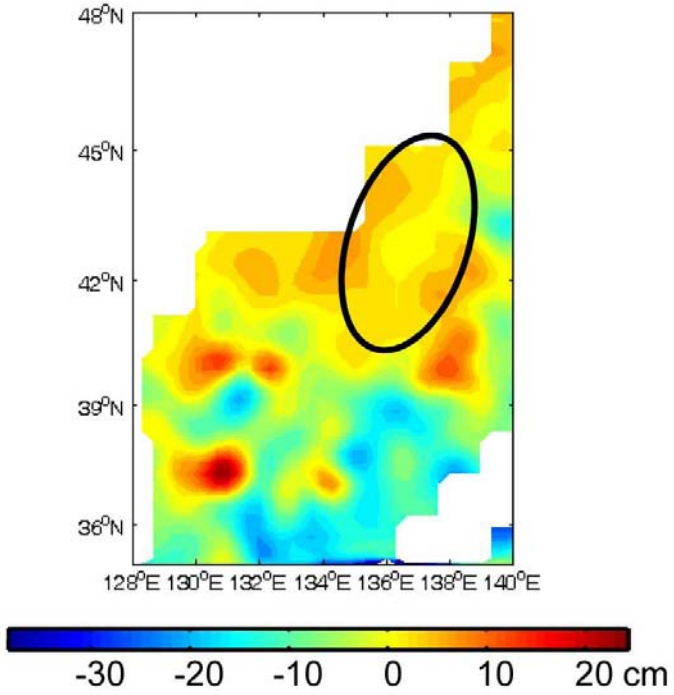

Figure 13 sea level anomaly from the AVISO merged (T/P+ERS2) product. The circled area is produced by the aliasing error from the combined aliasing from several neighboring and crossing tracks from Xu et al. (2008b).

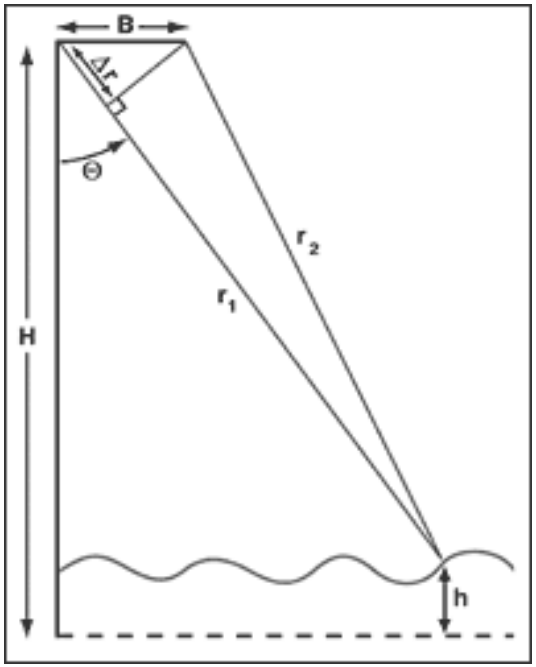

Figure 14 Geometric concept used for radar interferometry. Credit AVISO.

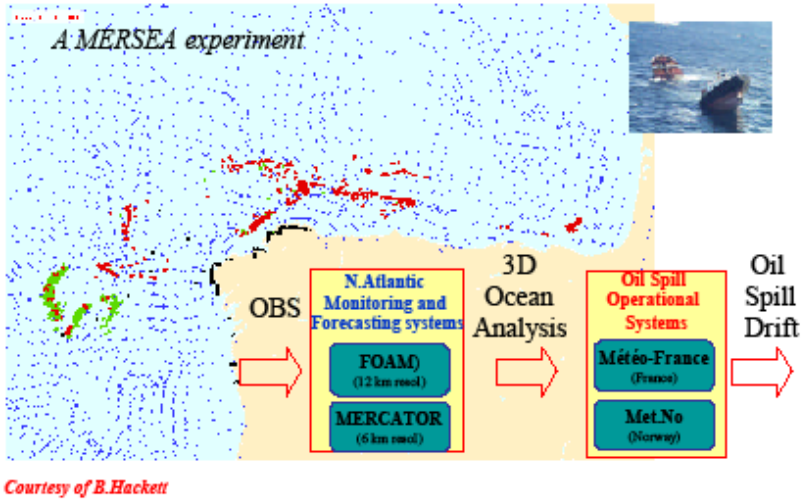

Figure 15 Operational oceanography applications: Marine Pollution (Prestige). The real time description and forecast of surface currents is not possible without a high resolution altimeter system. (credit Pierre-Yves Le Traon)